Enhancing the damping properties of cement mortar by pretreating coconut fibers for weakened interfaces

Tang, Zhen; Li, Zhenming; Hua, Jiang; Lu, Shuang; Chi, Lin

DOI
10.1016/j.jclepro.2022.134662

Publication date
2022

Document Version
Final published version

Published in
Journal of Cleaner Production

Citation (APA)
Tang, Z., Li, Z., Hua, J., Lu, S., & Chi, L. (2022). Enhancing the damping properties of cement mortar by pretreating coconut fibers for weakened interfaces. *Journal of Cleaner Production*, *379*, Article 134662. https://doi.org/10.1016/j.jclepro.2022.134662

Journal of Cleaner Production 379 (2022) 134662

Contents lists available at ScienceDirect

Journal of Cleaner Production

journal homepage: www.elsevier.com/locate/jclepro

Enhancing the damping properties of cement mortar by pretreating coconut fibers for weakened interfaces

Zhen Tang [a,b,1], Zhenming Li [c,1], Jiang Hua [a,b], Shuang Lu [a,b,*], Lin Chi [d,**]

[a] School of Civil Engineering, Harbin Institute of Technology, 150090, Harbin, China
[b] Key Lab of Structures Dynamic Behavior and Control of the Ministry of Education, Harbin Institute of Technology, Harbin, 150090, China
[c] Department of Materials, Mechanics, Management & Design, Delft University of Technology, Delft, 2628 CN, the Netherlands
[d] School of Environment and Architecture, University of Shanghai for Science and Technology, Shanghai, 200093, China

ARTICLE INFO

Handling Editor: Jiri Jaromir Klemeš

Keywords:
Coconut fiber
Pretreatment
Interface
Damping
Cement

ABSTRACT

Pretreated coconut fibers can be applied as renewable damping components in fiber-reinforced cement mortars to reduce the adverse effects of vibration and promote the recycling of waste fibers. In this study, FT-IR, TG, XRD, and SEM measurements were performed to analyze the morphologies and physicochemical properties of the coconut fibers before and after pretreatment. The compressive strength, porosity, and damping properties were tested to study the effects of fiber pre-treatment on the mechanical properties of cement mortar. In contrast to original fibers, pretreated coconut fibers induced a moderate air-entraining effect in cement mortars. Therefore, the mortars with pretreated fibers exhibited significantly lower strength loss, indicating consistency with the porosity results. Furthermore, by adding 0.75 vol% coconut fibers pretreated by a mixed solution of NaOH and H_2O_2, the loss tangent of the cement mortar can be increased by 25%. The enhanced damping properties were attributed to the weakened interface between the fibers and cement mortar matrix, which facilitated dissipation of the vibration energy. Moreover, a simplified shear-lag model was proposed to describe the relationship between the weakened interface frictional sliding and the damping properties of the cement mortars.

1. Introduction

Dynamic loads, such as earthquakes and winds, cause vibrations in the building structure, leading to safety and serviceability problems. The damage caused by vibrations can be mitigated by improving the damping performance of the structure (Liang et al., 2021; Tandazo et al., 2021). Installing vibration-damping devices can improve the damping performance and seismic resistance; however, such devices involve complex construction and high costs. Modification of the damping properties of cement-based materials is an alternative strategy to enhance the damping performance (Damiani et al., 2021; Lee et al., 2018; Li et al., 2018; Tang et al., 2022; Zheng et al., 2008).

Owing to the inherent friability and poor ductility of cement, sand, and stone, the damping properties of cement-based materials are difficult to improve by optimizing the mix ratio of these basic materials. Therefore, researchers have attempted to incorporate damping reinforcement materials into cements to increase dissipation energy under dynamic loads (Kulhavy et al., 2018; Li et al., 2017; Liew et al., 2017; Ruan et al., 2017). There are two strategies to increase the energy dissipation of cement-based materials. The first is to use viscoelastic polymers to increase the bulk viscoelasticity of a system (Atef et al., 2021; Romanazzi et al., 2021). The molecules or molecular segments of the incorporated viscoelastic polymers move under dynamic loads and dissipate the vibration energy (Chung, 2019). Rubber is a representative viscoelastic polymer. Its low glass-transition temperature ensures good viscoelasticity under the service temperature of cement-based materials. However, the application of viscoelastic polymers has been largely limited in cement-based materials because of the obvious loss of compressive strength and aging of the polymers (Park et al., 2022; Tan and Feyzullahoglu, 2021). For example, the damping ratio can be increased by 32.5% when 30% of sand is replaced by rubber, while the compressive strength is reduced by 30% (Moustafa and ElGawady, 2015).

Another energy-dissipation strategy is to increase the interface of the

* Corresponding author. School of Civil Engineering, Harbin Institute of Technology, 150090, Harbin, China.
** Corresponding author. School of Environment and Architecture, University of Shanghai for Science and Technology, Shanghai, 200093, China.
E-mail addresses: hitlu@126.com (S. Lu), chilin@usst.edu.cn (L. Chi).
[1] These authors contributed equally to this work.

https://doi.org/10.1016/j.jclepro.2022.134662
Received 11 May 2022; Received in revised form 7 October 2022; Accepted 10 October 2022
Available online 15 October 2022

system. The relative movement among the multiphase interfaces can generate heat through friction, dissipate energy, and improve the damping properties (Lai et al., 2019). Abundant weak interfaces are introduced by incorporating discontinuous or continuous fillers (Tian et al., 2020, 2021b). Specifically, discontinuous fillers, such as rice husk ash and graphene, are primarily microparticles or nanoparticles (Cong et al., 2021b; Long et al., 2018); continuous fibers include natural and artificial fibers (Ali et al., 2012; Saghafi and Shariatmadar, 2018; Tian et al., 2022; Yan et al., 2000). Frictional sliding at the interfaces between the fibers and cement matrix can consume vibration energy (Long et al., 2021). Natural fibers have more hydrophilic functional groups on the surfaces than artificial fibers. These functional groups have been confirmed to strengthen the interface, hindering frictional sliding and reducing the dissipation of vibration energy. Therefore, the application of natural fibers to enhance the damping properties of cement-based materials is limited (Yan et al., 2016). However, natural fibers have considerably lower costs than artificial fibers and are renewable and locally available in various countries (Ali et al., 2012). Therefore, finding suitable methods to weaken the bonding strength of natural fibers to enhance the damping properties is environmentally and economically beneficial, while avoiding a significant reduction in the static mechanical properties of cement-based materials.

Coconut fibers, extracted from the outer shell of coconuts, are typical natural fibers consisting of cellulose, hemicellulose, and lignin (Yadav et al., 2020). In previous studies, when coconut fibers were immersed in a NaOH solution, hemicellulose gradually degraded by the β-elimination reaction (Ferraz et al., 2011, 2012; Yan et al., 2016). Meanwhile, ether bonds, such as α-aryl ether and α-alkyl ether of lignin, were broken by the action of nucleophiles and other chemical reactions, increasing the surface roughness of the fibers and removing lignin. Moreover, during the alkali treatment process, the surfaces of the coconut fibers were gradually covered by the polysaccharide polymer gel, hindering the progress of the reaction. The combination of residual lignin and Ca^{2+} and the coarse surface of fibers strengthened the interface between the fibers and matrix, deferring the interface frictional sliding and vibration energy dissipation (Andic-Cakir et al., 2014; Asasutjarit et al., 2007; Oliveira et al., 2018). Under these circumstances, it is necessary to find a suitable method to remove lignin from the coconut fibers, thereby weakening the bond between the fibers and matrix. The chemical reaction between H_2O_2 and NaOH can produce HOO^-, which has strong oxidizing abilities to decompose lignin. Hence, H_2O_2 can work synergistically with NaOH to remove lignin, weaken the interface between the fibers and matrix, and improve the damping properties (Sedan et al., 2007).

In this study, a NaOH solution and a mixed solution of NaOH and H_2O_2 were used to pretreat the coconut fibers to remove lignin in the fibers and modify the interfaces between the fiber and cement matrix. Fourier-transform infrared spectrometry (FT-IR), X-ray diffraction (XRD), thermogravimetric analysis (TG), and scanning electron microscopy (SEM) were used to explore the variations in the morphology and physicochemical properties of the coconut fibers after pretreatment. The loss tangents, storage moduli, loss moduli, porosities, and compressive strengths of the cement mortars were tested to investigate the effects of coconut fibers on the properties of cement mortars. The interfaces were observed using SEM to explore the effect of the pretreatment methods on the fiber-matrix interface. A simplified shear-lag model was established to intuitively explain the mechanism of damping enhancement.

2. Materials and methods

2.1. Raw materials

P.O.42.5 ordinary Portland cement and quartz sand with a particle size between 0.212 and 0.380 mm were used in this study to prepare cement mortars. Coconut fiber with a length of less than 3 mm was purchased from Jiangxi Lifeng Hemp Industry Co., Ltd. A polycarboxylic acid superplasticizer (SP) was used. The coconut fibers were treated with NaOH and H_2O_2 (analytically pure) dissolved in deionized water.

2.2. Pretreatment of coconut fibers

The coconut fibers were dispersed using a low-speed crusher for 30 s. The obtained fibers were dispersed in a NaOH solution (2.5 wt %) or a mixed solution of NaOH (2.5 wt%) and H_2O_2 (1 wt%) and stirred at 80 °C for 3 h. The solid-to-liquid ratio was 1:25. The pretreated coconut fibers were washed and filtered repeatedly until the filtrate was neutral. Finally, the treated fibers were dried at 60 °C for 24 h. The original coconut fibers were named OCF. The coconut fibers pretreated with the NaOH solution were named NCF, and those pretreated with the mixed solution of NaOH and H_2O_2 were named NHCF. The images of the original and pretreated coconut fibers are shown in Fig. 1.

2.3. Cement mortar preparation

Nineteen cement mortars (including cement mortar with no fiber) were prepared with various fiber types (OCF, NCF, and NHCF) and volumes (0%, 0.25%, 0.5%, 0.75%, 1.0%, 1.25%, and 1.5%). The cement mortar proportions are listed in Table 1. Short fibers used in this study tend to agglomerate, which can impair the properties of the cement mortar. Hence, the mixing procedure was carefully designed and conducted as follows. Cement and coconut fibers were first mixed by a crusher at a low speed to assist fiber dispersion in the cement while restricting the damage to the fibers. After 30 s, the mixture and quartz sand were added to the mortar mixer and stirred for 2 min at a low speed. Water and SP were then added to the mixture. After 1 min, high-speed mixing was applied for 5 min. The obtained cement mortar was cast into a mold and demolded one day later. The mixing process and sequence are shown in Fig. 2. The demolded cement mortars were cured in a standard curing room (20 ± 1 °C and ≥95% RH) for 27 d.

2.4. Methodology

2.4.1. Characterization of original and pretreated coconut fibers

The original and pretreated coconut fibers were mixed with potassium bromide to prepare pellets for the FT-IR characterization in the wavenumber range of 4000–400 cm^{-1}.

The TG curves of coconut fibers were obtained using an SDT-650 analyzer in an N_2 environment. The temperature range was from room temperature to 1000 °C.

The crystallinity of the coconut fibers was characterized using a Rigaku D/Max-2600/PC X-ray diffractometer (XRD) with a 2θ scan range of 5–60°.

The dried and gold-sprayed coconut fibers were observed using a Quanta 200 FEG SEM with an accelerating voltage of 30 kV. The cement mortars were also tested using the same parameters.

The length and diameter of the fibers were calculated by measuring 300 fibers under an ultra-depth microscope.

The coconut fibers were dried to a constant weight and then placed in a humid environment (20 ± 1 °C and ≥95%RH). At 5, 10, 20, 30, 40, 50, 60, 80, 100, and 120 min, the weight of the sample was recorded. Moisture regain was calculated using Eq. (1).

Fig. 1. Pictures of original and pretreated coconut fibers.

Table 1
Mix proportion of cement mortar with coconut fibers.

Mix ID		Cement (g)	Sand (g)	OCF (g)	NCF (g)	NHCF (g)	Water (g)
CM		600	900	0.00			270
OCF-CM	OCF-0.25	600	900	2.74	–	–	270
	OCF-0.5			5.47	–	–	
	OCF-0.75			8.21	–	–	
	OCF-1.0			10.95	–	–	
	OCF-1.25			13.68	–	–	
	OCF-1.5			16.42	–	–	
NCF-CM	NCF-0.25	600	900	–	2.83	–	270
	NCF-0.5			–	5.66	–	
	NCF-0.75			–	8.49	–	
	NCF-1.0			–	11.33	–	
	NCF-1.25			–	14.16	–	
	NCF-1.5			–	16.99	–	
NHCF-CM	NHCF-0.25	600	900	–	–	2.86	270
	NHCF-0.5			–	–	5.71	
	NHCF-0.75			–	–	8.57	
	NHCF-1.0			–	–	11.42	
	NHCF-1.25			–	–	14.28	
	NHCF-1.5			–	–	17.13	

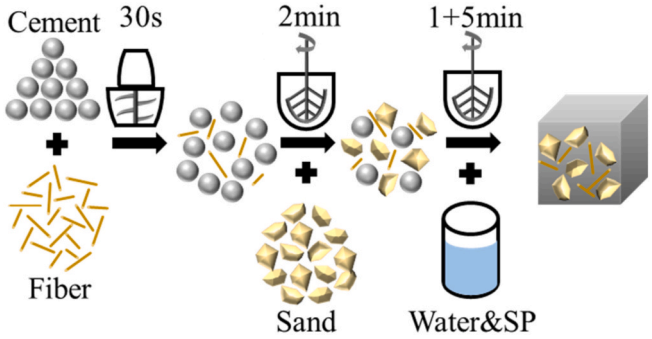

Fig. 2. Preparation process of cement mortar.

$$Moisture\ regain(\%) = \frac{m_t - m_0}{m_t} \quad (1)$$

where m_t and m_0 are the weights of the sample at t and 0 min, respectively.

The density of the coconut fibers was measured using the pycnometer method. The mass of the empty pycnometer (100 mL) was recorded as m_1. Thereafter, the fiber was added to the pycnometer, and the mass m_2 was recorded. Deionized water was added to the pycnometer. After standing for 2 h, the pycnometer was completely filled with deionized water, and the mass m_3 was recorded. The density of the fibers was calculated using Eq. (2).

$$density\left(g/cm^3\right) = \frac{m_2 - m_1}{m_3 - m_1 - 100 \times \rho_{water}} \quad (2)$$

2.4.2. Porosity of the cement mortars

The mass of the dried specimen was recorded as m_a. The mass of the specimen saturated with water under vacuum was recorded as m_b. The water-saturated specimen was suspended in water, and the mass was recorded as m_c. According to ASTM C642-13, the porosities of the cement mortars were calculated using Eq. (3).

$$porosity = \frac{m_b - m_a}{m_b - m_c} \quad (3)$$

2.4.3. Static mechanical tests

The compressive strengths of the cement mortar mixtures were measured. The loading speed was 2400 N/s. The average compressive strength was obtained by testing six samples of dimensions 40 mm × 40 × 40 mm^3.

2.4.4. Dynamic mechanical analysis

The process for dynamic mechanical analysis is shown in Fig. 3. Cement mortars with dimensions of 4 mm × 12 × 60 mm^3 were tested using a Q800 dynamic mechanical analyzer. The test frequency was 1 Hz, and the amplitude was 5 μm. The damping properties (loss tangent, storage modulus, and loss modulus) were determined by testing three cement mortars.

3. Properties of original and pretreated coconut fibers

3.1. Chemical bonds

The FT-IR spectra of the original and pretreated coconut fibers are shown in Fig. 4. The adsorption peaks and their corresponding chemical bonds and sources are listed in Table 2. The absorption peak at 2852 cm^{-1} is attributed to CH_2 symmetrical stretching from the wax. Only OCF presents an adsorption peak at 2852 cm^{-1}, while no obvious peaks are observed in the spectra of NCF and NHCF, indicating that the wax in the coconut fibers is removed after the treatment (Le Troedec et al., 2008). NCF and NHCF exhibit weaker absorption peaks at 1643 cm^{-1} and 1242 cm^{-1} than OCF, which are related to the C–C aromatic ring structure and C–O aryl group, respectively. The above results indicate that lignin is effectively removed by the NaOH solution and the mixed solution of NaOH and H_2O_2 (Haque et al., 2020; Le Troedec et al., 2008).

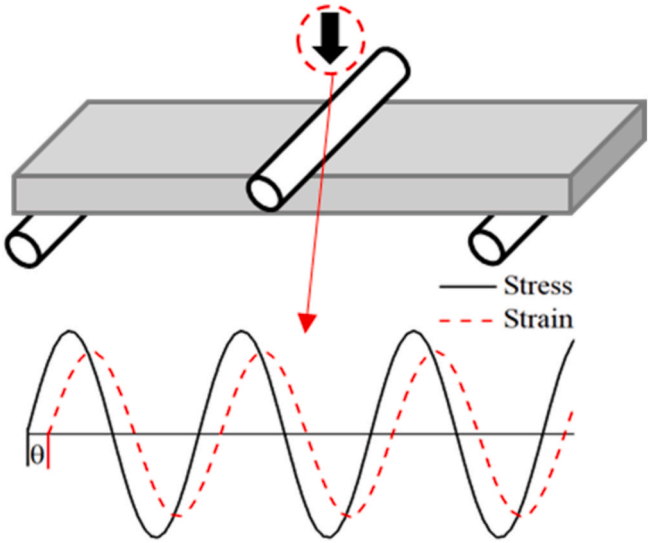

Fig. 3. Test process of dynamic mechanical analysis.

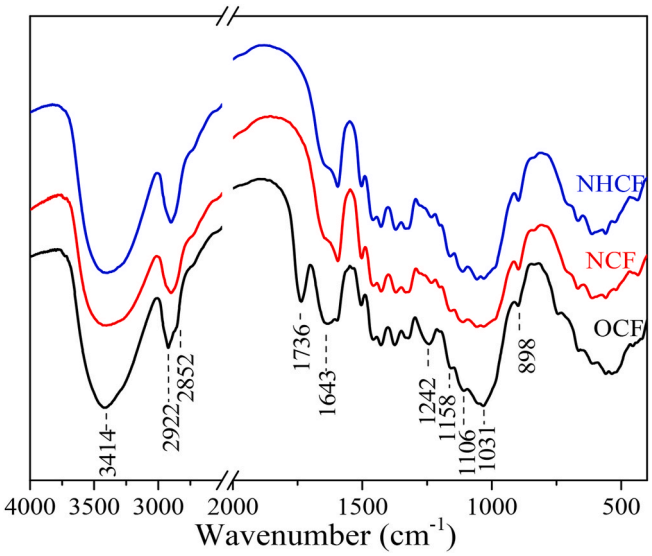

Fig. 4. FT-IR spectra of the original and pretreated coconut fibers.

Table 2
Infrared adsorption frequencies of coconut fibers (Haque et al., 2020; Jayaramudu et al., 2009; Le Troedec et al., 2008; Rong et al., 2001).

Wavenumber (cm^{-1})	Vibration	Source
3414	O–H stretching	α-cellulose
2922	C–H stretching	Cellulose and hemicellulose
2852	CH_2 symmetrical stretching	Wax
1736	carbonyl band unconjugated stretching	Hemicellulose
1643	C–C aromatic ring structure	Lignin
1242	C–O aryl group	Lignin
1158	C–O–C asymmetric stretching	Cellulose and hemicellulose
1106	C–C-O stretching	Cellulose and hemicellulose
1031	C-O stretching	Cellulose, hemicellulose, and lignin
898	C–O–C stretching	Hemicellulose and cellulose

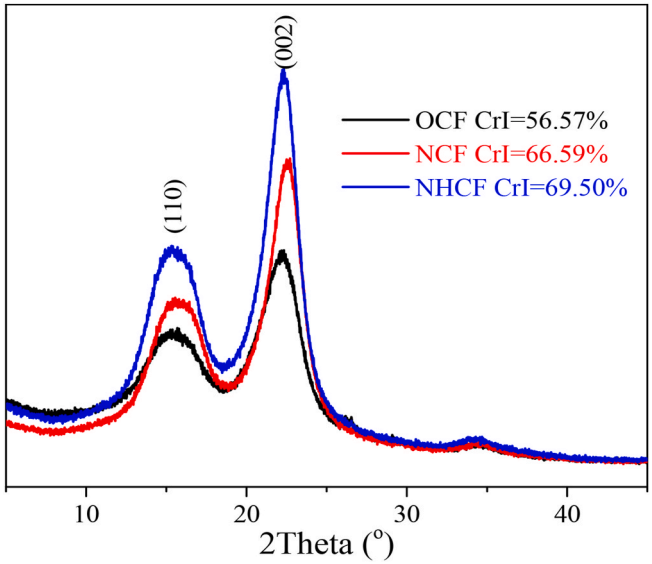

Fig. 5. XRD patterns of the original and pretreated coconut fibers.

3.2. Relative crystallinity

Fig. 5 shows the XRD patterns of the original and pretreated coconut fibers. The relative crystallinity of the coconut fibers was calculated using Eq. (4).

$$CI = \frac{I_{002} - I_{am}}{I_{002}} \times 100\% \quad (4)$$

where *CI* is relative crystallinity. I_{002} is the diffraction intensity of the (002) peak. I_{am} is the diffraction intensity of the amorphous region (Moshi et al., 2020).

The relative crystallinities of OCF, NCF, and NHCF are 56.57%, 66.59%, and 69.50%, respectively. Cellulose has a crystal structure, while lignin and hemicellulose are amorphous. The *CI* values of NCF and NHCF are higher than that of OCF, indicating the degradation and dissolution of non-cellulose components (hemicellulose and lignin) in the pretreatment process. The *CI* of NHCF is higher than that of NCF, confirming that H_2O_2 is more beneficial for removing amorphous structures.

3.3. Thermostability

Fig. 6 shows the DTG-TG analysis results of the original and pretreated coconut fibers. All three fibers exhibited excellent thermal stability below 200 °C. Unlike NCF and NHCF, OCF shows a significant weight loss at approximately 284.9 °C, which is related to the decomposition of lignin and hemicellulose (Prasad et al., 2018). This result further confirms that both lignin and hemicellulose are effectively removed by the NaOH solution or the mixed solution of NaOH and H_2O_2 (Fan et al., 2021). The temperatures at the maximum weight loss rates of OCF, NCF, and NHCF are observed at 356.8 °C, 365.6 °C, and 366.0 °C, respectively. The gradual increase in degradation temperature is owing to the less amorphous components and higher relative crystallinity (Basu et al., 2015).

3.4. Microscopic morphology

As a filling and binding substance, lignin can bond and strengthen cellulose fibers both physically and chemically. Therefore, removing lignin breaks the tight connections between cellulose fibers, resulting in more fiber bifurcation. In addition, less lignin reduced the brown color of the coconut fibers. As shown in Fig. 1(a) and (b), the color of NCF is lighter than that of OCF, indicating that part of the lignin is removed by the NaOH solution, consistent with the analysis results shown in Figs. 4–6 (Mononen et al., 2005). As shown in Fig. 7(a) and (b), the

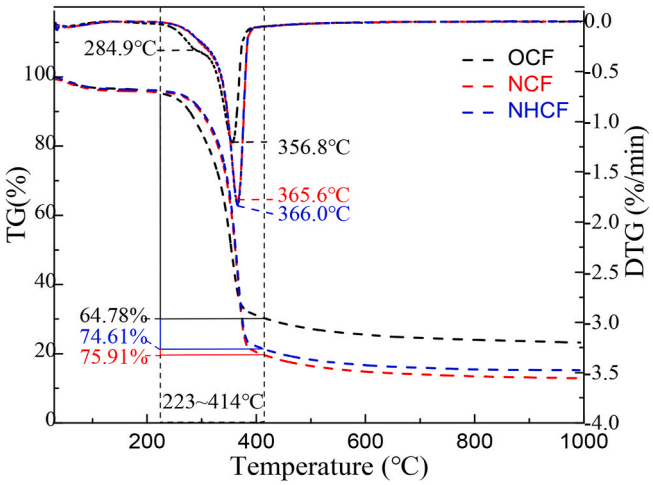

Fig. 6. DTG-TG analysis of the original and pretreated coconut fibers.

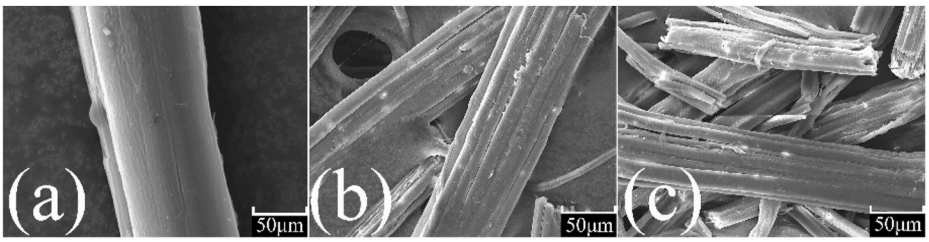

Fig. 7. SEM images of original and pretreated coconut fibers.

surface of the OCF is smooth, and the cellulose fibers in the OCF are tightly combined through the lignin. However, owing to the lack of lignin, gaps are observed between the cellulose fibers in NCF and structural deterioration and bifurcation are found in NHCF (Fig. 7(c)). The color gradually became lighter from NCF to NHCF, confirming that H_2O_2 is more conducive to removing lignin, consistent with the above FT-IR, XRD, and TG results.

3.5. Physical properties

Pretreatment modifies the composition and structure of coconut fibers, which determines their physical properties. As shown in Fig. 8(a) and Table 3, the diameter of OCF (47.263 μm) is smaller than those of NCF (63.952 μm) and NHCF (56.393 μm), and the aspect ratio of OCF (17.133) is larger than those of NCF (14.429) and NHCF (13.275 μm). The NaOH solution or the mixed solution of NaOH and H_2O_2 can remove lignin, destructing the tight connections among cellulose fibers. The impaired connection among the cellulose fibers further induces gaps and increases the diameters of the coconut fibers. Moreover, the swelling effect is weakened due to the synergistic effect of H_2O_2 and NaOH, and the coconut fibers bifurcate and even peel off (Fig. 7). Based on the above discussion, it is clear that the diameter of the NHCF is smaller than that of the NCF.

Moisture regain is an indicator of water absorption of the fibers, which is closely related to the working performance of the fresh fiber mortar. The amounts of cellulose, hemicellulose, and lignin in the three fibers are different. However, these substances have various hydrophilic functional groups and good hydrophilicity, and there is no significant difference between the moisture regain (9.343–10.06%) of the original and pretreated coconut fibers. Therefore, the difference in the water absorption performance of the coconut fibers has a negligible effect on the working performance of the fresh mortar under the same fiber dosage.

Table 3
Physical properties of the original and pretreated coconut fibers.

	Moisture regain (2 h, %)	Density (g/cm^3)	Length (Avg, μm)	Diameter (Avg, μm)	Aspect ratio (Avg)
OCF	9.638	1.330	775.446	47.263	17.133
NCF	9.343	1.376	766.526	63.952	14.429
NHCF	10.066	1.387	700.815	56.393	13.275

The coconut fiber content in cement-based materials is usually calculated based on its volume ratio, which is reflected by the density results. The pretreatment process can remove low-density lignin and increase the crystallinity and density of the cellulose. As shown in Table 3, the density of the coconut fibers gradually increases from 1.330 g/cm^3 (OCF) to 1.387 g/cm^3 (NHCF).

4. Effects on cement mortar properties

4.1. Porosity

The porosities of the cement mortars containing the original and pretreated coconut fibers are shown in Fig. 9. The maximum porosities of OCF-1.5, NCF-1.25, and NHCF- NHCF-1.5 were 90.47%, 12.64%, and 34.38% higher than that of CM. The coconut fibers (with or without pretreatment) play an air-entraining role in the mortar. Among the three coconut fibers, the OCF had the most significant air-entraining effect. Specifically, the porosity of OCF-CM was higher than that of NCF-CM, indicating that NaOH treatment can reduce the air-entraining effect of the coconut fibers. Compared with OCF, the rougher surface of NCF

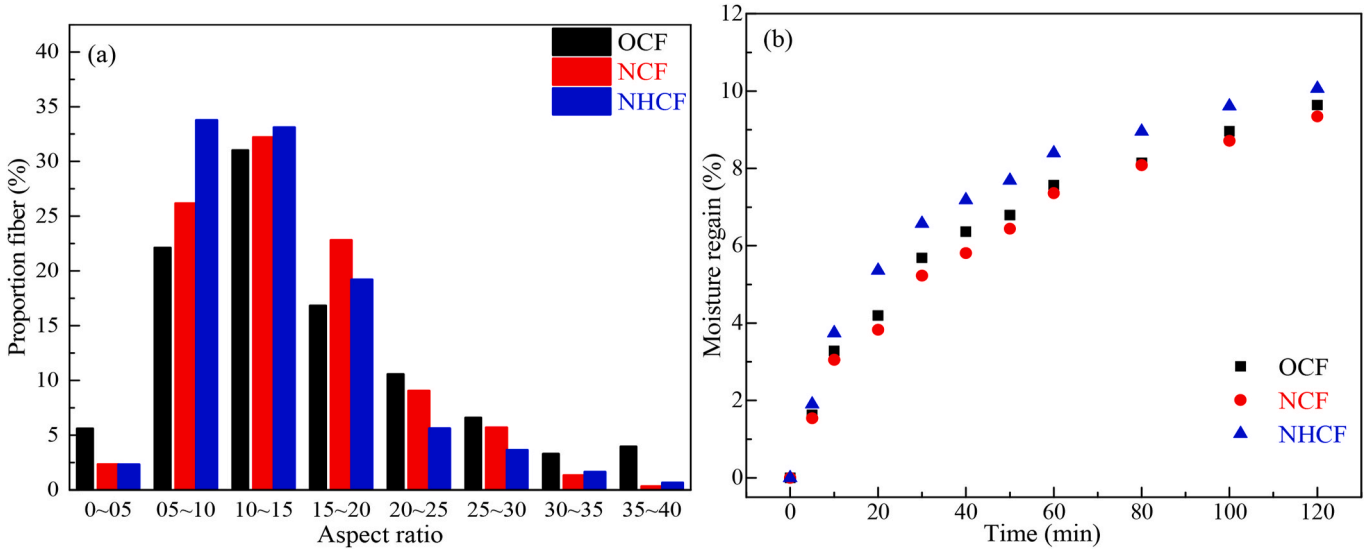

Fig. 8. Aspect ratio (a) and moisture regain (b) of the original and pretreated coconut fibers.

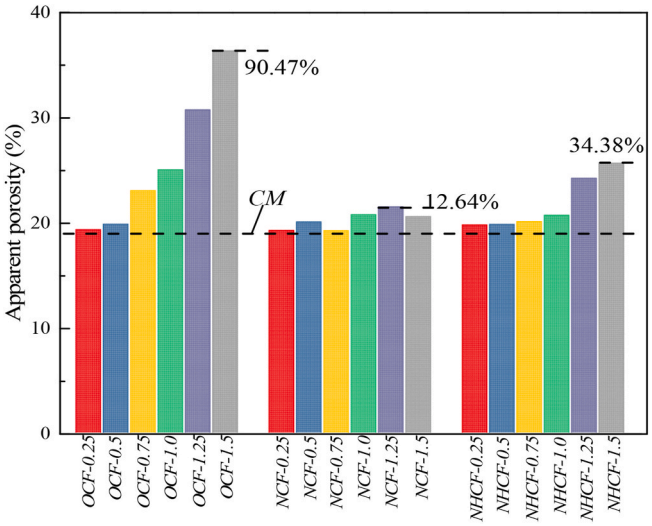

Fig. 9. Porosity of cement mortar.

(Fig. 7) is more favorable for a closer bond between the fiber and matrix (Chikouche et al., 2015; Gouveia Guedes et al., 2021). Furthermore, the air-entraining effect of the coconut fiber can also be reduced by the mixed solution of NaOH and H_2O_2, and the air-entraining effect of NHCF was more obvious than that of NCF (34.38% vs. 12.64%). The detailed effects of H_2O_2 and NaOH solutions will be discussed in Section 4.4.

4.2. Compressive strength

As shown in Fig. 10, the compressive strength of cement mortar is reduced by incorporating OCF, and adding more OCF causes a lower compressive strength of OCF-CM. The compressive strengths of OCF-0.5 and OCF-1.5 were 25.82% and 71.44% lower than that of CM, respectively. In contrast, a small amount of NCF and NHCF in the cement mortar can improve its compressive strength. The compressive strengths of NCF-0.5 and NHCF-0.5 are 8.32% and 4.46% higher than that of CM, respectively. However, the compressive strengths are reduced when more NCF and NHCF are introduced. The compressive strengths of NCF-1.5 and NHCF-1.25 are 35.32% and 49.61% lower than that of CM, respectively. The cement mortars containing NCF and NHCF show a less significant decrease in compressive strength than the mortar containing OCF. Moreover, the compressive strength increases with a small amount of pretreated coconut fibers, indicating the importance of pretreatment.

Adding coconut fibers can change the porosity, which is critical for compressive strength (Chi et al., 2022). To study the relationship between compressive strength and porosity, the Ryshkewitch empirical formula, Eq. (5), was used (Matusinovic et al., 2003).

$$\delta_c = \delta_0 e^{-\alpha P} \tag{5}$$

where δ_c and P are the compressive strength and porosity of the sample, respectively. δ_0 is the compressive strength of the sample with zero porosity and α is the empirical constant. The correlation coefficient (R^2) of the Ryshkewitch empirical formula is 0.8128, confirming that the compressive strength is more related to the porosity rather than the type of coconut fibers.

4.3. Dynamic mechanical analysis

As shown in Fig. 3, when the cement mortar is subjected to sinusoidal alternating stress, the dynamic strain lags the dynamic stress, indicating that the cement mortar has a certain degree of viscoelasticity. The relationships among the dynamic mechanical properties, stress, and strain are expressed in Eq. (6) ~ (9).

$$\sigma(t) = \sigma_0 \sin \omega t \tag{6}$$

$$\varepsilon = \varepsilon_0 \sin(\omega t - \theta) \tag{7}$$

$$\frac{\sigma(t)}{\varepsilon(t)} = \frac{\sigma_0 \sin \omega t}{\varepsilon_0(\sin \omega t - \theta)} = \frac{\sigma_0}{\varepsilon_0}(\cos\theta + i\sin\theta) = E' + E'' \tag{8}$$

$$\eta = \tan\theta = \frac{E''}{E'} \tag{9}$$

where σ_0 and ε_0 are the maximum stress and strain amplitudes, respectively. The loss tangent angle (θ) is the phase difference between stress and strain, and ω is the angular frequency. η is loss tangent. E' and E'' are the storage and loss moduli, respectively.

The damping properties (loss tangent, loss modulus, and storage modulus) of the cement mortar were evaluated via dynamic mechanical analysis. The storage modulus is an index relevant to stiffness and rep-

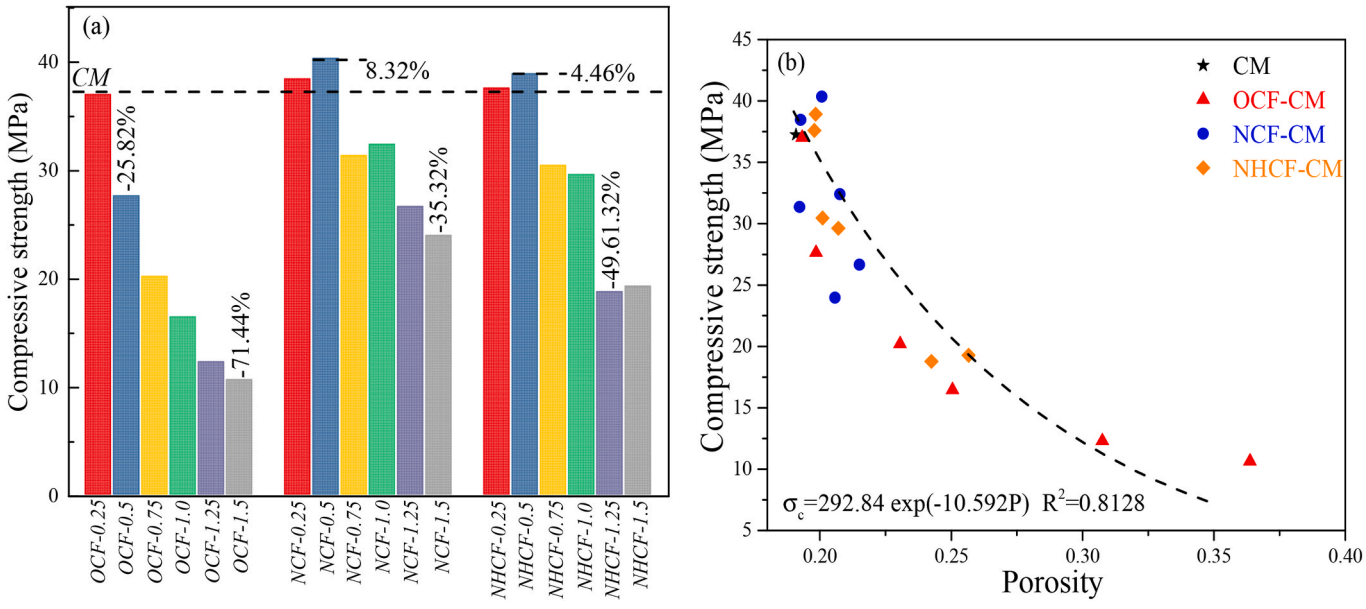

Fig. 10. (a) Compressive strength of cement mortar and (b) Relationship between compressive strength and porosity.

resents the energy absorption in the elastic range (Cong et al., 2021a). The relationship between E', the cement mortar matrix, and the coconut fibers is shown in Eq. (10).

$$\frac{1}{2}\varepsilon_0^2 \mathrm{E}^{'} = W_m V_M + W_f V_f + W_{mf} \tag{10}$$

where W_m and W_f are the strain energies of the cement mortar matrix and coconut fibers, respectively. V_m and V_f are the volume fractions of the cement mortar matrix and coconut fibers, respectively. W_{mf} is the energy dissipated at the interface between the cement and fibers.

The storage modulus of coconut fibers is lower than that of cement mortar; therefore, E' decreases when V_f increases. As mentioned above, all three coconut fibers have air-entraining effects in the cement mortar matrix, decreasing W_m and E'. Therefore, as shown in Fig. 11(a), with the increase in V_f, the storage modulus of the cement mortar with pretreated coconut fibers exhibits a different reducing regularity. The E' of OCF-1.25 is 43.78% lower than that of CM; however, the E' values of NCF-1.25 and NHCF-1.25 are 32.25% and 34.15% lower than that of CM, respectively, indicating the benefits of the pretreatment of coconut fibers.

The loss modulus represents the energy lost as dissipated heat during a cyclic load. As shown in Fig. 11(b), the maximum loss moduli of NCF-0.75 and NHCF-0.75 increase by 3.77% and 12.12%, respectively, compared to that of CM. The loss modulus of cement mortar cannot be improved by OCF and NCF, whereas incorporating NHCF can improve the loss modulus effectively, indicating the importance of the synergistic effects of NaOH and H_2O_2 on the coconut fibers.

The loss tangent is an indicator of the damping capability of cement mortar. As shown in Fig. 11(c), the loss tangent of cement mortar containing coconut fibers is generally higher than that of CM. Compared with CM, the maximum loss tangents of OCF-0.75, NCF-0.75, and NHCF-0.75 increased by 16.86%, 12.00%, and 25.45%, respectively, indicating that the damping properties can be improved by incorporating coconut fibers. The damping improvement by adding 0.75% vol. % NHCF in cement mortar can reach 80% of the improvement when 30% vol. % rubber is used, indicating the excellent effect of coconut fiber. Multiple

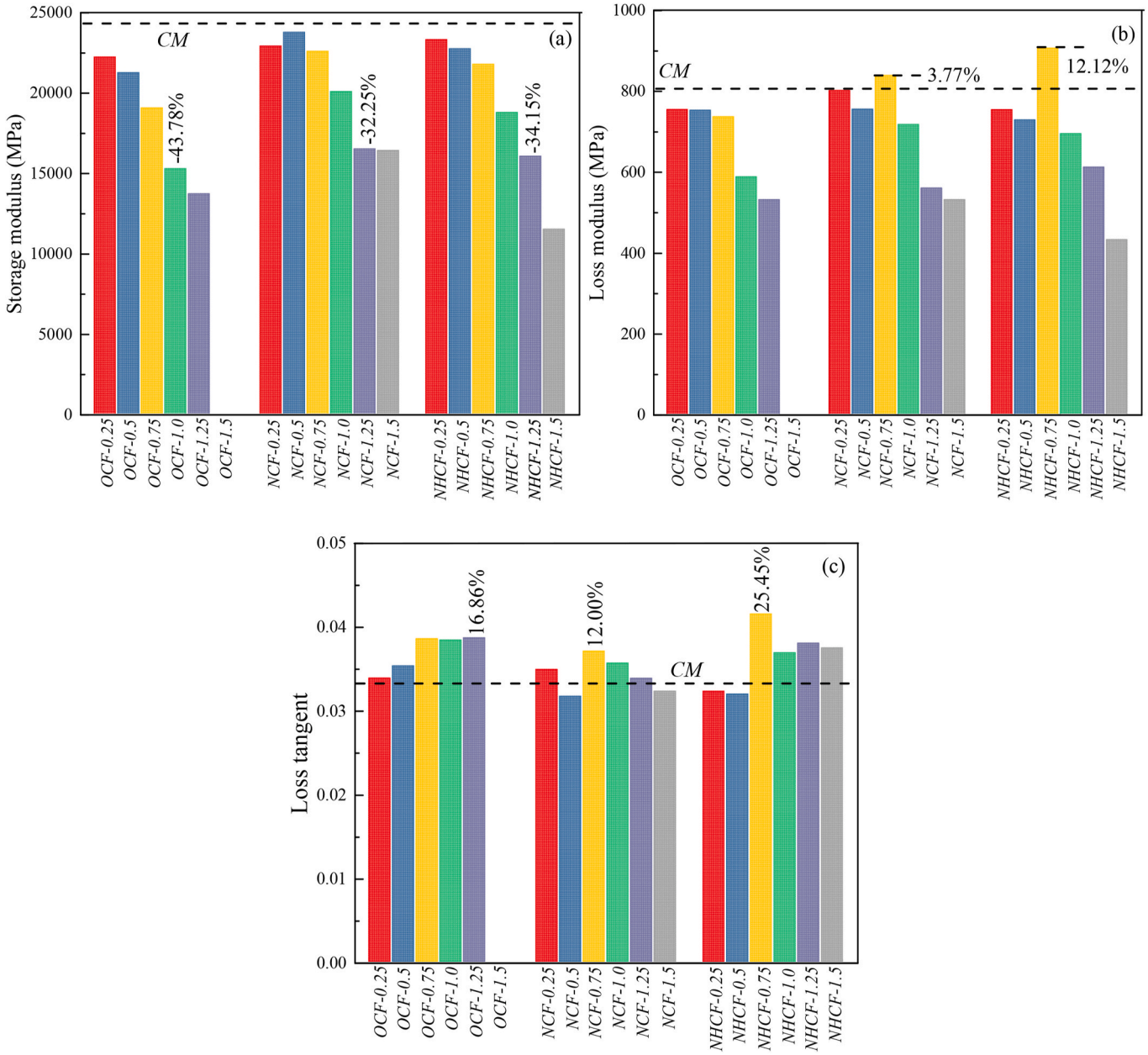

Fig. 11. (a) Storage modulus; (b) Loss modulus, and (c) Loss tangent of cement mortar.

interfaces and pores generated by incorporating coconut fibers can dissipate the vibration energy. The maximum loss tangent of OCF-CM is higher than that of NCF-CM but lower than that of NHCF-CM, implying that NaOH solution alone cannot improve the damping properties, whereas the pretreatment using the mixed solution of NaOH and H_2O_2 is more effective.

To further clarify the impact of pores and fibers on the damping properties of cement mortar, the maximum loss tangent of each sample group and the corresponding porosity were compared (Fig. 12). The porosity of NCF-0.75 only increased by 0.71% compared with CM, while the loss tangent of NCF-0.75 increased by 12.00%, indicating that incorporating fibers can improve the damping properties of cement mortar. Compared with CM, the porosities of OCF-0.75 and OCF-1.25 increased by 20.73% and 61.05%, respectively. However, the increases in the loss tangent of OCF-0.75 and OCF-1.25 are almost the same (16.50% and 16.48%, respectively), indicating the porosity has a limited effect on damping properties. Compared with OCF-0.75, NHCF-0.75 has lower porosity and higher loss tangent, suggesting that incorporating suitable fibers can improve the damping properties more effectively than introducing pores. The influence of different fibers on damping properties is discussed below.

4.4. SEM images analysis

As shown in Fig. 13, various interactions occur between coconut fibers and cement hydration products. The surface of OCF is attached to most hydration products, whereas the surface of NHCF has a few hydration products. The amount of hydration products on the surface of NCF is between those of OCF and NHCF, and the hydration products not only grow on the NCF surface in situ but also penetrate NCF. The bonding situation between different fibers and the matrix is closely related to the contents of lignin and cellulose in the three coconut fibers.

A schematic of the bonding situation between the coconut fibers and cement hydration products is shown in Fig. 14. Cellulose has a very low calcium affinity, whereas the dissolution of lignin under alkaline conditions can generate carboxyl and phenolic hydroxyl groups to combine with Ca^{2+} (Fu et al., 2014). The bond between lignin and Ca^{2+} mineralizes the fiber, triggering in-situ the growth of hydration products on the fibers (Melo Filho et al., 2013; Teixeira et al., 2020). Among the three fibers, OCF with the most lignin generates the most hydration products in OCF-CM. The gaps between the cellulose fibers of NCF were penetrated by the cement pore solution, resulting in the formation of hydration products inside the fibers. Compared with OCF and NCF, NHCF contains the least amount of lignin; therefore, the surface of NHCF is rarely attached to the hydration products. The bond between NCF and the matrix is tighter than that between NHCF and the matrix, explaining that the porosity of NHCF-CM is generally higher than that of NCF-CM.

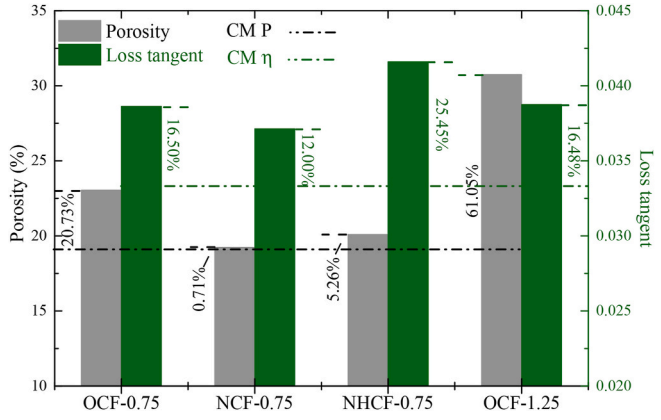

Fig. 12. Relationship between porosity and loss tangent.

4.5. Cement mortar matrix-fibers shear lag model

To explain the influence mechanism of the original and pretreated coconut fibers on the damping properties of the cement mortars, a simplified shear lag model was established and shown in Fig. 15. The cement mortar matrix and coconut fibers were simplified into cylinders with radii r_m and r_f, respectively. σ_{fx} and ε_{fx} are the stress and strain of the fibers at distance x from the midpoint of the fibers, respectively. σ_{mx} and ε_{mx} are the stress and strain of the cement mortar matrix at the corresponding positions, respectively. τ_{fx} is the interfacial stress at distance x from the midpoint of the fibers. $\sigma_0 sin\omega t$ is the sinusoidal alternating stress applied to the cement mortar.

The relationships among r_m, r_f, σ_{fx}, ε_{fx}, x, σ_{mx}, ε_{mx}, τ_{fx}, and $\sigma_0 sin\omega t$ are given by Eq. 11–14.

$$2\pi r_f \tau_{fx} = \pi r_f^2 \sigma_{fx} \tag{11}$$

$$r_f^2 \sigma_{fx} + \pi\left(r_m^2 - r_f^2\right)\sigma_{mx} = \sigma_0 \sin \omega t \tag{12}$$

$$\varepsilon_{fx} = \sigma_{fx} E_f \tag{13}$$

$$\varepsilon_{mx} = \sigma_{mx} E_m \tag{14}$$

where E_f and E_m are the elasticity modulus of fibers and cement mortar matrix, respectively.

The damping properties are achieved through energy dissipation due to interface frictional sliding, which is calculated using Eq. (15). The interface energy dissipation is closely related to the length of the debonding zone of the fibers (τ_{fx}, ε_{fx}, and ε_{mx}). By substituting Eqs. (11)–(14) into Eq. (15), the interface energy-dissipation formula is given by Eq. (16).

$$W_{mf} = \int 2\pi r_f \tau_{fx}\left(\varepsilon_{fx} - \varepsilon_{mx}\right)dx \tag{15}$$

$$W_{mf} = 2\pi r_f \int \tau_{fx}\left(\frac{2\tau_{fx}}{r_f E_f} - \frac{\sigma_0 \sin \omega t - 2\pi r_f \tau_{fx}}{\pi\left(r_m^2 - r_f^2\right)E_m}\right)dx \tag{16}$$

The length of the debonding zone of the fibers ($\int dx$) is critical for the bonding between the coconut fibers and the matrix. In this study, different pretreatments change the bonding, decreasing or increasing the length of the debonding zone. As shown in Figs. 14 and 15, the mineralized areas on NHCF are smaller than those on NCF and OCF. A continued weak interface is constructed between the NHCF and cement mortar matrix, which can increase the length of the debonding zone of the fibers and effectively dissipate the vibration energy (Li, 2021). Therefore, NHCF has the best effect on improving the damping properties of cement mortar. However, OCF and NCF are attached to various hydration products and form strong bonds with the cement mortar matrix, preventing the fibers from debonding from the cement mortar matrix and hindering the dissipation of vibration energy (Zhang et al., 2020).

In addition to $\int dx$, the relationship between τ_{fx} and the breaking strength of the fibers cannot be ignored. When the volume fractions of NHCF are small in the NHCF-CM, the loss tangents of NHCF-0.25 and NHCF-0.5 are approximately the same as that of CM, indicating that incorporating a small amount of NHCF fails to improve the damping properties. This is because τ_{fx} is related to the volume fraction of fibers, elastic modulus, stress of the cement mortar, etc. With a small amount of NHCF, τ_{fx} is larger than the breaking strength of the NHCF. Fibers are broken instead of being pulled out from the cement mortar matrix under the action of a sinusoidal alternating force. The vibration energy dissipated by fiber breakage is limited and cannot improve the damping properties. Interface frictional sliding is more conducive to energy consumption than fiber breakage (Tonoli et al., 2012). As shown in Fig. 10(a), the lower compressive strength of NHCF-0.75 indicates that

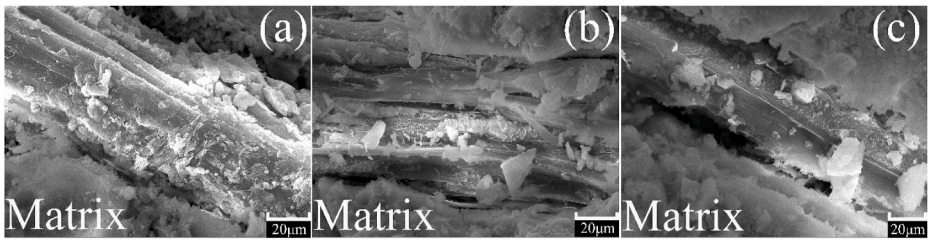

Fig. 13. SEM images of (a) OCF-CM, (b) NCF-CM, (c) NHCF-CM.

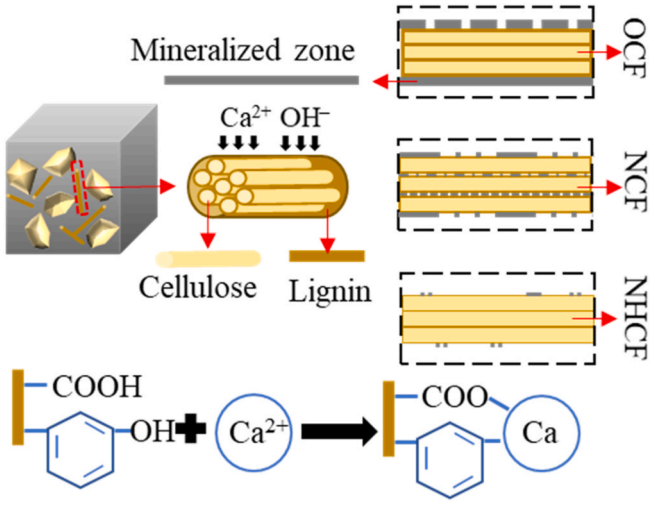

Fig. 14. Schematic of the bondings between coconut fibers and cement hydration products.

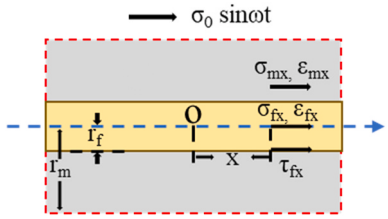

Fig. 15. Cement mortar matrix-fibers shear lag model.

the compactness of the matrix is lower than those of NHCF-0.25 and NHCF-0.5. Therefore, the decreased τ_{fx} of NHCF-0.75 suggests that NHCF can be pulled out from the cement mortar matrix, resulting in vibration energy dissipation by interface frictional sliding. Therefore, the loss tangent of NHCF-0.75 is higher than those of NHCF-0.25 and NHCF-0.5.

4.6. Sustainability analysis

Statistics from the Food and Agriculture Organization of the United Nations indicate that global coconut fiber production in 2020 is approximately 1,276,624 tons (Food and Agriculture Data, 2020). In this study, coconut fiber was used as a damping reinforcement material, enabling large-scale and high-value-added applications of the fiber.

As an industrial product, the damping mortar needs to be manufactured at low cost. The dosage of each material per cubic meter was calculated according to the mix proportions (Table 1), and bulk densities of CM (1940 kg/m^3) and NFCF-0.75 (1750 kg/m^3). The cost of each material was calculated based on the prices of materials in the Chinese market (Prices of main building materials for highway engineering, 2022; Water price information, 2022; Pitarch et al., 2021). The raw material dosage and costs per cubic meter for CM and NHCF-0.75. are listed in Table 4. Water^1 and Water^2 are the dosages of water used in the preparation of cement mortar and treatment of coconut fiber, respectively.

As shown in Table 4, the total material cost per cubic meter of NHCF-0.75 (872.26 CNY) is lower than that of CM (921.95 CNY). Furthermore, to comprehensively evaluate the dynamic mechanical properties and economic cost of the cement mortar, the cost per unit loss tangent was compared. The cost/tanθ value of NHCF-0.75 (20967.84 CNY/m^3) is 25.49% lower than that of CM (27803.12 CNY/m^3). These results indicate that using pretreated coconut fiber for damping reinforcement has excellent economic benefits. In addition, environmental benefits must also be considered. Cement manufacturing is the main source of CO_2 emissions for building materials (Tian et al., 2021a). CO_2 emissions per ton of cement are as high as 750 kg (Pitarch et al., 2021). The cement consumption per cubic meter of NHCF-0.75 was 10.23% lower than that of CM. The CO_2 emissions of cement per cubic meter of NHCF-0.75 are 50.45 kg less than that of CM, which is significantly higher than the carbon emissions of other materials combined (Long et al., 2022). As discussed above, the economic and environmental costs of NHCF-0.75 are lower than those of CM, indicating that the cement mortar containing pretreated coconut fiber has the potential for extensive engineering applications.

5. Conclusion

In this study, the damping properties of cement mortar were improved by incorporating renewable coconut fibers before and after different treatments. FT-IR, XRD, TG, and SEM were used to characterize the treated fibers. The compressive strength, porosity, and damping properties of the cement mortar were tested. SEM images and a simplified shear-lag model were used to explain the damping properties. The conclusions are summarized as follows:

(1) The lignin in coconut fibers could be reduced by a NaOH solution and further removed by a mixed solution of NaOH and H_2O_2. The bonding between coconut fibers and cement hydration products was modified to produce weakened interfaces by pretreating coconut fibers with a mixed solution of NaOH and H_2O_2.

Table 4
Cost and dosage of each raw material to manufacture CM and NHCF-0.75/m.^{3}.

Components	Unit price (CNY/Kg)	CM		NHCF-0.75	
		Dosage (kg/m^3)	Cost (CNY)	Dosage (kg/m^3)	Cost (CNY)
Cement	0.50	657.63	328.82	590.36	295.18
Sand	0.6	986.44	591.86	885.54	531.32
Water^1	0.0043	295.93	1.27	265.66	1.14
Fiber	3	–	–	8.43	25.19
NaOH	2.5	–	–	5.27	13.17
H_2O_2	1.2	–	–	2.11	2.53
Water^2	0.0043	–	–	843	3.62
Total	–	–	921.95	–	872.26

(2) The porosities of OCF-1.5, NCF-1.25, and NHCF-1.5 were 90.47%, 12.64%, and 34.38% higher than that of CM, respectively, indicating that the air-entraining effect of the coconut fibers was effectively reduced by pretreatment. The compressive strength loss was also reduced by pretreatment. The loss tangents of OCF-0.75, NCF-0.75, and NHCF-0.75 were 16.86%, 12.00%, and 25.45% higher than those of CM, respectively, indicating the advantage of using a mixed solution of NaOH and H_2O_2.
(3) The mechanism of damping enhancement is discussed using a simplified shear-lag model, which further illustrates the relationship between the interface and damping properties. The damping properties of cement mortar can be improved through the weakened interfaces when they undergo frictional sliding.

CRediT authorship contribution statement

Zhen Tang: Formal analysis, Data curation, Methodology, Validation, Writing – original draft. **Zhenming Li:** Writing – review & editing, Methodology, Validation. **Jiang Hua:** Investigation, Data curation, Project administration. **Shuang Lu:** Conceptualization, Supervision, Validation, Writing – review & editing, Funding acquisition. **Lin Chi:** Conceptualization, Supervision, Validation, Writing – review & editing, Funding acquisition.

Declaration of competing interest

The authors declare that they have no known competing financial interests or personal relationships that could have appeared to influence the work reported in this paper.

Data availability

Data will be made available on request.

Acknowledgments

This research was funded by the National Natural Science Foundation of China (No. 51872064, No. 52178196 and No. 52208269), State Key Laboratory of Solid waste Reuse for Building Materials (No. SWR-2020-005, Beijing building materials academy of science research, China), and Shanghai Sailing Program (No.20YF1431800).

References

Ali, M., Liu, A., Sou, H., Chouw, N., 2012. Mechanical and dynamic properties of coconut fibre reinforced concrete. Construct. Build. Mater. 30, 814–825.
Andic-Cakir, O., Sarikanat, M., Tufekci, H.B., Demirci, C., Erdogan, U.H., 2014. Physical and mechanical properties of randomly oriented coir fiber-cementitious composites. Compos. B Eng. 61, 49–54.
Asasutjarit, C., Hirunlabh, J., Khedari, J., Charoenvai, S., Zeghmati, B., Shin, U.C., 2007. Development of coconut coir-based lightweight cement board. Construct. Build. Mater. 21 (2), 277–288.
Atef, M., Bassioni, G., Azab, N., Abdellatif, M.H., 2021. Assessment of cement replacement with fine recycled rubber particles in sustainable cementitious composites. J. Mech. Behav. Mater. 30 (1), 59–65.
Basu, G., Mishra, L., Jose, S., Samanta, A.K., 2015. Accelerated retting cum softening of coconut fibre. Ind. Crop. Prod. 77, 66–73.
Chi, L., Li, W., Li, Z., Wang, Z., Lu, S., Liu, Q., 2022. Investigation of the hydration properties of cement with EDTA by alternative current impedance spectroscopy. Cem. Concr. Compos. 126.
Chikouche, M.D.L., Merrouche, A., Azizi, A., Rokbi, M., Walter, S., 2015. Influence of alkali treatment on the mechanical properties of new cane fibre/polyester composites. J. Reinforc. Plast. Compos. 34 (16), 1329–1339.
Chung, D.D.L., 2019. Interface-derived solid-state viscoelasticity exhibited by nanostructured and microstructured materials containing carbons or ceramics. Carbon 144, 567–581.
Cong, X., Tang, Z., Lu, S., Tan, Y., Wang, C., Yang, L., Shi, X., 2021a. Effect of rice husk ash surface modification by silane coupling agents on damping capacity of cement-based pastes. Construct. Build. Mater. 296, 123730.
Cong, X., Tang, Z., Lu, S., Tan, Y., Wang, C., Yang, L., Shi, X., 2021b. Effect of rice husk ash surface modification by silane coupling agents on damping capacity of cement-based pastes. Construct. Build. Mater. 296.
Damiani, R.M., Mondal, P., Lange, D.A., 2021. Mechanical performance of rubberized cement paste with calcium sulfoaluminate cement addition. Construct. Build. Mater. 266, 120790.
Fan, F., Zhu, M., Fang, K., Xie, J., Deng, Z., Wang, X., Zhang, Z., Cao, X., 2021. Comparative study on enhanced pectinase and alkali-oxygen degummings of sisal fibers. Cellulose 28 (13), 8375–8386.
Ferraz, J.M., Del Menezzi, C.H.S., Teixeira, D.E., Martins, S.A., 2011. Effects of treatment of coir fiber and cement/fiber ratio on properties of cement-bonded composites. Bioresources 6 (3), 3481–3492.
Ferraz, J.M., Del Menezzi, C.H.S., Souza, M.R., Okino, E.Y.A., Martins, S.A., 2012. Compatibility of pretreated coir fibres (Cocos nucifera L.) with Portland cement to produce mineral composites. Int. J. Polym. Sci. 2012, 290571.
Food and Agriculture Data, 2020. Food and Agriculture Organization of the United Nations assessed 20 Augsust 2022). https://www.fao.org/faostat/zh/#data.
Fu, L.-H., Ma, M.-G., Bian, J., Deng, F., Du, X., 2014. Research on the formation mechanism of composites from lignocelluloses and CaCO3. Mater. Sci. Eng. C-Mater. Biol. Appl. 44, 216–224.
Gouveia Guedes, C.E., de Oliveira, D.N.P.S., Bezerra, J.B., Oliveira Penido, C.A.F.d., Ferreira, N.S., Lustrino Borges, W., Bufalino, L., Souza, T.M., 2021. Exploiting the Amazonian acai palm leaves potential as reinforcement for cement composites through alkali and bleaching treatments. J. Nat. Fibers. https://doi.org/10.1080/15440478.15442021.11941483.
Haque, M.A., Ashik, M.A., Aktar, S., Akter, M.S., Halilu, A., Haque, M.A., Islam, M.R., Abdullah-Al-Mamun, M., Nahar, M.N.-E.N., Das, S.R., Das, K.C., Ahmed, I., Manir, M. S., Islam, M.K., Shahadat, M.R.B., 2020. Rapid Deconstruction of Cotton, Coir, Areca, and Banana Fibers Recalcitrant Structure Using a Bacterial Consortium with Enhanced Saccharification. Waste Biomass Valorization, pp. 4001–4018.
Jayaramudu, J., Guduri, B.R., Rajulu, A.V., 2009. Characterization of natural fabric Sterculia urens. Int. J. Polym. Anal. Char. 14 (2), 115–125.
Kulhavy, P., Samkova, A., Petru, M., Pechociakova, M., 2018. Improvement of the acoustic attenuation of plaster composites by the addition of short-fibre reinforcement. Adv. Mater. Sci. Eng. 2018, 7356721.
Lai, P., Zhi, X., Shen, S., Wang, Z., Yu, P., 2019. Strength and damping properties of cementitious composites incorporating original and alkali treated flax fibers. Appl. Sci.-Basel 9 (10).
Le Troedec, M., Sedan, D., Peyratout, C., Bonnet, J.P., Smith, A., Guinebretiere, R., Gloaguen, V., Krausz, P., 2008. Influence of various chemical treatments on the composition and structure of hemp fibres. Compos. Appl. Sci. Manuf. 39 (3), 514–522.
Lee, K.S., Choi, J.-I., Park, S.E., Hwang, J.-S., Lee, B.Y., 2018. Damping property of prepacked concrete incorporating coarse aggregates coated with polyurethane. Cem. Concr. Compos. 93, 301–308.
Li, L., 2021. A micromechanical temperature-dependent vibration damping model of fiber-reinforced ceramic-matrix composites. Compos. Struct. 261.
Li, W., Ji, W., Isfahani, F.T., Wang, Y., Li, G., Liu, Y., Xing, F., 2017. Nano-Silica sol-gel and carbon nanotube coupling effect on the performance of cement-based materials. Nanomaterials 7 (7), 185.
Li, T., Xiao, J., Sui, T., Liang, C., Li, L., 2018. Effect of recycled coarse aggregate to damping variation of concrete. Construct. Build. Mater. 178, 445–452.
Liang, C., Xiao, J., Wang, C., Ma, Z., He, Z., 2021. Frequency-Dependent damping properties of recycled aggregate concrete. J. Mater. Civ. Eng. 33 (7), 04021160.
Liew, K.M., Kai, M.F., Zhang, L.W., 2017. Mechanical and damping properties of CNT-reinforced cementitious composites. Compos. Struct. 160, 81–88.
Long, W.-J., Wei, J.-J., Xing, F., Khayat, K.H., 2018. Enhanced dynamic mechanical properties of cement paste modified with graphene oxide nanosheets and its reinforcing mechanism. Cem. Concr. Compos. 93, 127–139.
Long, W.-J., Li, H.-D., Mei, L., Li, W., Xing, F., Khayat, K.H., 2021. Damping characteristics of PVA fiber-reinforced cementitious composite containing high-volume fly ash under frequency -temperature coupling effects. Cem. Concr. Compos. 118, 103911.
Long, W.-J., Wu, Z., Khayat, K.H., Wei, J., Dong, B., Xing, F., Zhang, J., 2022. Design, dynamic performance and ecological efficiency of fiber-reinforced mortars with different binder systems: ordinary Portland cement, limestone calcined clay cement and alkali-activated slag. J. Clean. Prod. 337.
Matusinovic, T., Sipusic, J., Vrbos, N., 2003. Porosity-strength relation in calcium aluminate cement pastes. Cement Concr. Res. 33 (11), 1801–1806.
Melo Filho, J.d.A., Silva, F.d.A., Toledo Filho, R.D., 2013. Degradation kinetics and aging mechanisms on sisal fiber cement composite systems. Cem. Concr. Compos. 40, 30–39.
Mononen, K., Alvila, L., Pakkanen, T.T., 2005. Changes in color and structure of birch wood (Betula pendula) caused by bleaching with hydrogen peroxide solution. Holzforschung 59 (1), 59–64.
Moshi, A.M.A., Ravindran, D., Bharathi, S.S.R., Indran, S., Priyadharshini, S.G., 2020. Characterization of surface-modified natural cellulosic fiber extracted from the root of Ficus religiosa tree. Int. J. Biol. Macromol. 156, 997–1006.
Moustafa, A., ElGawady, M.A., 2015. Mechanical properties of high strength concrete with scrap tire rubber. Construct. Build. Mater. 93, 249–256.
Oliveira, L.A., Santos, J.C., Panzera, T.H., Freire, R.T.S., Vieira, L.M.G., Scarpa, F., 2018. Evaluation of hybrid-short-coir-fibre-reinforced composites via full factorial design. Compos. Struct. 202, 313–323.
Park, H.Y., Kim, T.H., Kim, D.Y., Seo, K.H., Kang, D.G., Kim, H.Y., Lee, D.Y., 2022. Influence of blend ratio on long-term thermal aging and oil resistance in fluorosilicone/silicone rubber. Polym.-Korea 46 (1), 127–134.
Pitarch, A.M., Reig, L., Tomás, A.E., Forcada, G., Soriano, L., Borrachero, M.V., Payá, J., Monzó, J.M., 2021. Pozzolanic activity of tiles, bricks and ceramic sanitary-ware in eco-friendly Portland blended cements. J. Clean. Prod. 279.

Prasad, N., Agarwal, V.K., Sinha, S., 2018. Thermal degradation of coir fiber reinforced low-density polyethylene composites. Sci. Eng. Compos. Mater. 25 (2), 363–372.
Water price information, 2022. Harbin Water Supply Group Co., LTD assessed 20 Augsust 2022). https://web.hrbgongshui.com/about/?135.html.
Prices of main building materials for highway engineering, 2022. Transportation Department of Heilongjiang Province assessed 20 Augsust 2022. http://www.hljjt.gov.cn/z_gczjglzz/sglgczjglzz_cljg/2022/08/17837.html.
Romanazzi, V., Leone, M., Tondolo, F., Fantilli, A.P., Aiello, M.A., 2021. Bond strength of rubberized concrete with deformed steel bar. Construct. Build. Mater. 272, 121730.
Rong, M.Z., Zhang, M.Q., Liu, Y., Yang, G.C., Zeng, H.M., 2001. The effect of fiber treatment on the mechanical properties of unidirectional sisal-reinforced epoxy composites. Compos. Sci. Technol. 61 (10), 1437–1447.
Ruan, Y., Zhou, D., Sun, S., Wu, X., Yu, X., Hou, J., Dong, X., Han, B., 2017. Self-damping cementitious composites with multi-layer graphene. Mater. Res. Express 4 (7), 075605.
Saghafi, M.H., Shariatmadar, H., 2018. Enhancement of seismic performance of beam-column joint connections using high performance fiber reinforced cementitious composites. Construct. Build. Mater. 180, 665–680.
Sedan, D., Pagnoux, C., Chotard, T., Smith, A., Lejolly, D., Gloaguen, V., Krausz, P., 2007. Effect of calcium rich and alkaline solutions on the chemical behaviour of hemp fibres. J. Mater. Sci. 42 (22), 9336–9342.
Tan, B., Feyzullahoglu, E., 2021. The investigation of effects of environmental conditions on fatigue strength and spring stiffness of rubber materials. J. Elastomers Plastics 53 (6), 632–652.
Tandazo, C.M.V., Tu, J., Gao, K., 2021. Research on vibration control for glass fiber reinforced polymer reinforced concrete (GFRP RC) frames subject to seismic loading. Compos. Struct. 261, 113290.
Tang, Z., Li, G., Lu, S., Wang, J., Chi, L., 2022. Enhance mechanical damping behavior of RHA-cement mortar with bionic inorganic-organic laminated structures. Construct. Build. Mater. 323, 126521.
Teixeira, J.N., Silva, D.W., Vilela, A.P., Savastano Junior, H., de Siqueira Brandão Vaz, L. E.V., Mendes, R.F., 2020. Lignocellulosic materials for fiber cement production. Waste Biomass Valorization 11 (5), 2193–2200.
Tian, W., Wang, M., Liu, Y., Wang, W., 2020. Ohmic heating curing of high content fly ash blended cement-based composites towards sustainable green construction materials used in severe cold region. J. Clean. Prod. 276.
Tian, W., Liu, Y., Wang, M., Wang, W., 2021a. Performance and economic analyses of low-energy ohmic heating cured sustainable reactive powder concrete with dolomite powder as fine aggregates. J. Clean. Prod. 329.
Tian, W., Liu, Y., Wang, W., 2021b. Multi-structural evolution of conductive reactive powder concrete manufactured by enhanced ohmic heating curing. Cem. Concr. Compos. 123.
Tian, W., Liu, Y., Wang, W., 2022. Enhanced ohmic heating and chloride adsorption efficiency of conductive seawater cementitious composite: effect of non-conductive nano-silica. Compos. B Eng. 236, 109854.
Tonoli, G.H.D., Belgacem, M.N., Bras, J., Pereira-da-Silva, M.A., Rocco Lahr, F.A., Savastano, H., 2012. Impact of bleaching pine fibre on the fibre/cement interface. J. Mater. Sci. 47 (9), 4167–4177.
Yadav, K.K., Singh, H., Rana, S., , Sunaina, Sammi, H., Nishanthi, S.T., Wadhwa, R., Khan, N., Jha, M., 2020. Utilization of waste coir fibre architecture to synthesize porous graphene oxide and their derivatives: an efficient energy storage material. J. Clean. Prod. 276, 124240.
Yan, L., Jenkins, C.H., Pendleton, R.L., 2000. Polyolefin fiber-reinforced concrete composites - Part I. Damping and frequency characteristics. Cement Concr. Res. 30 (3), 391–401.
Yan, L., Chouw, N., Huang, L., Kasal, B., 2016. Effect of alkali treatment on microstructure and mechanical properties of coir fibres, coir fibre reinforced-polymer composites and reinforced-cementitious composites. Construct. Build. Mater. 112, 168–182.
Zhang, W., Wu, P., Zhang, Y., Zeng, W., Yang, F., 2020. The effect of carbon nanotubes on the mechanical and damping properties of macro-defect-free cements. Sci. Eng. Compos. Mater. 27 (1), 28–40.
Zheng, L., Huo, X.S., Yuan, Y., 2008. Experimental investigation on dynamic properties of rubberized concrete. Construct. Build. Mater. 22 (5), 939–947.